Photodissociation dynamics of S_4N_4 at 222 and 248 nm

Andrew P. Ongstad,[a] Robert I. Lawconnell, [b] and Thomas L. Henshaw
Frank J. Seiler Research Laboratory, United States Air Force Academy, Colorado Springs, Colorado 80840-6528

(Received 30 September 1991; accepted 10 April 1992)

Emission from several electronically excited states of *NS* is observed when the energetic molecule S_4N_4 is photolyzed with radiation from an excimer laser. Photolysis at 248 nm generates fluorescence from the $B\,^2\Pi_{1/2,3/2}$, $H\,^2\Pi_{1/2}$, $G\,^2\Sigma^-$, and $I\,^2\Sigma^+$ states of NS. NS($B\,^2\Pi_{1/2,3/2}$) and NS($C\,^2\Sigma^+$) fluorescence is observed when the photolysis wavelength is changed to 222 nm. The NS(H) and NS(C) spectra are postulated to arise from a resonant interaction between the KrF and KrCl excimer photons, respectively, and vibrationally hot ground state NS. LIF excitation scans on the NS $X\,^2\Pi_{1/2,3/2} \rightarrow B\,^2\Pi_{1/2,3/2}$ system confirm the production of rotationally and vibrationally excited NS(X) up to $v''=4$. A mechanism, based on the experimental data (i.e., spectral composition, laser fluence studies, excited state time histories), calculated heats of formation, and Gaussian molecular orbital calculations, is proposed to account for the observed emissions. For photolysis at 248 nm it is hypothesized that a two photon absorption promotes the ground singlet state of S_4N_4 to an upper repulsive singlet state, which rapidly dissociates ($\tau \ll 30$ ns), producing an acyclic S_3N_3 fragment and vibrationally excited monomeric NS(X). The photofragments can interact further with the excimer radiation to produce NS(B) and NS(H), respectively. A similar mechanism is proposed to account for the presence of the NS(B) and NS(C) excited states for the 222 nm photolysis.

I. INTRODUCTION

The nitrogen sulfide radical is an unstable radical which cannot be stored as a monomeric liquid or solid, and must be produced *in situ* in the gas phase. NS is isoelectronic with NO and PO, and as expected, it shares many analogous states with these diatomics. For example, the NS $B\,^2\Pi$ and $C\,^2\Sigma^+$ electronic states have the well-known NO $B\,^2\Pi$ and $A\,^2\Sigma^+$ electronic states as their analogs, respectively. In both molecules, these states give rise to the β and γ band emission, respectively. However, the NO β bands lie significantly higher in energy (approximately 40 000 cm^{-1}) than the NS($B\,^2\Pi$) which lie near 30 000 cm^{-1}. The γ bands of both molecules are nearly resonant in energy, lying near 43,000 cm^{-1}.

Practical investigations involving NS are not nearly as numerous as the isovalent nitric oxide, which is known to play key roles in both combustion and atmospheric chemistry. However, the radical has been detected in atmospheric pressure flames by LIF methods,[1] and it has been detected in interstellar clouds via radio frequency emission.[2,3] The suggestion has also been made that NS may act as the active gain media in an electronic transition laser.[4,5] Specifically, the NS($B\,^2\Pi$) state of the molecule has been characterized as an attractive upper laser level primarily due to its significant Franck–Condon shift with respect to the NS ground state potential well.

Fluorescent emissions from NS are typically generated by reacting active nitrogen with a sulfur compound (e.g., H_2S, S_2Cl_2, SCl_2) in a discharge flow reactor. Such emissions have produced a wealth of spectroscopic and kinetic data. For example, the spectroscopy of the $B\,^2\Pi$ state has been well characterized with detailed measurements of Franck–Condon factors,[6] r centroids,[7] vibrational transition probabilities,[8] and perturbations.[9] Collisional quenching and vibrational energy transfer rates have also been measured for several collider gases.[10,11] Less information is available on the higher lying doublet states (e.g., $A\,^2\Delta$, $H\,^2\Pi$, $C\,^2\Sigma^+$), although studies utilizing pulsed laser techniques have begun to detail the spectroscopy of these more energetic states.[8] In this regard, we have recently reported on the KrF laser photolysis of the inorganic cage compound tetrasulfur tetranitride.[12] S_4N_4 may be regarded as a labile polymer composed of four thiazyl (NS) units (see inset to Fig. 1).[13] The photolysis produced fluorescent emission from several of the more energetic NS states including the $H\,^2\Pi_{1/2}$, $G\,^2\Sigma^-$, and $I\,^2\Sigma^+$. Strong NS($B\,^2\Pi$) emission was also observed, and measurements indicated the overall efficiency of conversion of absorbed photons by S_4N_4 into NS($B\,^2\Pi$) was $2.6\% \pm 0.7\%$. The facile photodecomposition process observed at 248 nm may be attributed to the energetic nature of S_4N_4 [ΔH_f(solid) = 110 kcal mol^{-1}],[14] the molecules large absorption cross section at 250 nm ($\sigma = 4.8 \times 10^{-17}$ cm^2), and the excellent energy overlap of the KrF excimer laser with the 250 nm absorption band.

This study extends and supplements our initial investigation, and we report on further measurements at the 248 nm photolysis wavelength, our LIF studies on the production of ground state NS(X), and on the fluorescent emission and products observed in the photolysis at 222 nm. A mechanism, based on the experimental observations (spectral composition, excited state time histories, fluence stud-

[a] Present address: Phillips Laboratory/LIDA, Kirtland Air Force Base, Albuquerque, New Mexico 87117.
[b] Present address: Mathematics Department, USAFA, Colorado 80840.

 0021-9606/92/141053-12$006.00

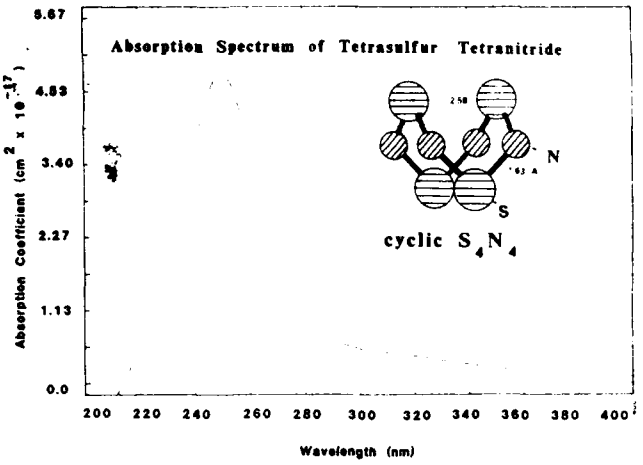

FIG. 1. UV–visible absorption spectrum of 2.92×10^{-5} M S_4N_4 in acetonitrile. The inset figure shows the cage like structure of S_4N_4.

ies, etc.), thermochemistry, and *ab initio* calculations, is proposed to account for the observed excited state and ground state products.

II. EXPERIMENT

The experimental apparatus consists of three general sections including the photolysis chamber, the detection ensemble, and the photolysis and probe lasers.

The photolysis chamber is constructed from a cylindrical piece of aluminum tubing 25 cm in length with an inside diameter of 3.5 cm. MgF_2 windows glued to the tubes end allow for the transmission of the laser radiation. LIF emissions originating within the cell were viewed off axis, at the cells center through MgF_2 windows. The S_4N_4 (typically $\leqslant 1$ g) was contained in a small 10 ml pyrex flask, which was connected to the chamber through a 12 mm side port. Nichrome wire wrapped around the neck of the flask, and a small heating mantle placed underneath the flask allowed for gentle heating/increased sublimation of the S_4N_4. Recrystalization of the tetramer on the cell surfaces was prevented by wrapping the cell with heating tape and heating the surface to near 70 °C. Flow through the cell was generated by a mechanical pump whose free air displacement was 500 l min^{-1}. To insure a new fill of S_4N_4 on every laser shot a flow of uhp helium buffer gas sufficient to flush the cell every 0.1 s was introduced slightly upstream of the S_4N_4 reservoir. The temperature of the He bath gas, measured at the center of the cell, was near 65 °C. The total pressure in the photolysis zone was measured with a capacitance manometer and was maintained in the range 0.8 to 1.2 Torr. The pressures of sublimed S_4N_4 were typically $\leqslant 10$ mTorr. Helium flow rates were measured with a calibrated mass flow meter.

The NS radicals produced in the photolysis were monitored by recording the LIF excitation spectrum of the $X\,^2\Pi \rightarrow B\,^2\Pi$ transition using a Nd:YAG pumped pulsed dye laser (PDL) with attendant frequency doubling. The bandwidth of the frequency doubled radiation was near 0.01 nm. Pulse energies $\leqslant 100$ μJ/pulse were employed in the LIF scans.

Photolysis of S_4N_4 was carried out with a excimer laser operated on KrF (248 nm) or KrCl (222 nm). The full-width at half maximum (FWHM) pulse width of this laser was 1 nm. The fluence of the excimer laser was varied from 1–85 mJ cm^{-2}. The PDL could be delayed from 0.5 to 255 μs from the photolysis pulse. The actual minimum delay was limited to ~ 2 μs due to the presence of prompt NS(B) fluorescence. The photolysis and probe lasers were arranged to counter propagate through the gas medium, the cross section of the photolysis beam being much larger than that of the probe beam. The LIF was filtered and detected by either a 1P28 or a R1463-01 photomultiplier tube (PMT), with the latter tube specific for photon counting. The signals from the PMT were sent, without amplification, straight to a gated photon counter operated in the boxcar mode. The photon counter was interfaced to a 80286 personal computer for data collection and manipulation. The spectral response of the dye laser/filter/PMT combination was measured, and used to correct the LIF excitation spectra. Spectra of the prompt emissions produced by the photolysis were recorded by replacing the bandpass filter with a 0.5 m monochromator. Alternatively, prompt emissions were dispersed with a 0.25 m polychromator and detected with a 1024 element silicon diode array. Calibration of the systems spectral sensitivity was performed with an Optronics Laboratory deuterium lamp and standard lamp.

The time histories of the emissions were collected with a 100 MHz oscilloscope which was interfaced via a GPIB to the 80286 PC. Storage and manipulation of the temporal traces were performed with Asystant/GPIB software.

S_4N_4 was prepared by reacting sulfur(II)chloride with NH_3 in CCl_4 solution, according to the method given by Villena-Blanco and Jolly.[15] The S_4N_4, formed in the reaction

$$6SCl_2 + 16NH_3 \rightarrow S_4N_4 + 2S + 12NH_4Cl,$$

was isolated by a soxhlet extraction with dry dioxane. On cooling large orange S_4N_4 crystals appeared, which were filtered and dried in air. The purity of the material was checked by FTIR and uv-vis. and indicated no appreciable impurities aside from traces of sulfur. A typical uv-vis. spectrum of S_4N_4 in acetonitrile is given in Fig. 1, and shows one primary unresolved vibronic band centered near 250 nm and a secondary much less intense feature (~ 310 nm) to the red of the primary. The main uv band at 250 nm has been attributed to either an $n \rightarrow \pi^*$ transition in NS[16] or to a $\sigma \rightarrow \sigma^*$ transition in the S–S interaction.[17] The 250 nm band has a large absorption cross section of 4.8×10^{-17} cm^2. Deeper in the uv, an additional strong absorption is observed close to 185 nm. The gas[12] and solution phase spectra are nearly identical.

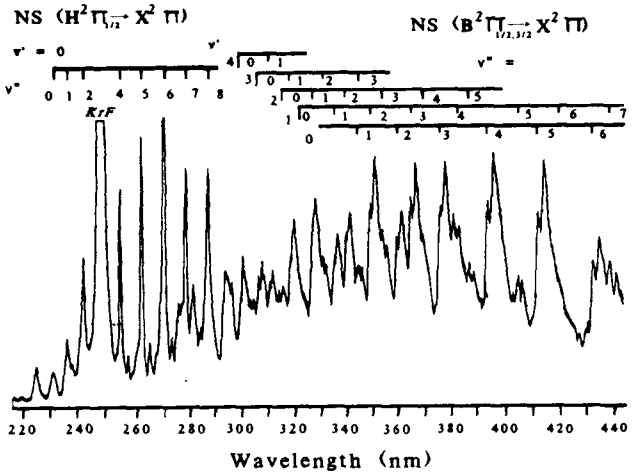

FIG. 2. Emission spectrum produced at the 248 nm photolysis wavelength. The broad band near 248 nm is due to the KrF laser spike.

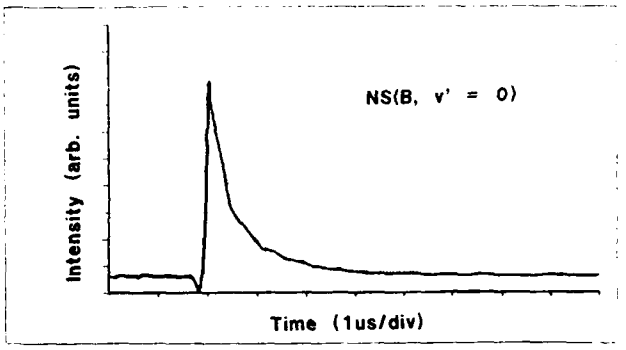

FIG. 3. Temporal profile of the NS($B \rightarrow X$) emission.

III. RESULTS

A. Photolysis at 248 nm

On photolysis of ~10 mTorr of S_4N_4 a bright blue emission was clearly visible to the eye. Figure 2 shows the spectrum of this prompt emission collected with the 0.25 m polychromator/diode array assembly. The emission extends from the uv (~200 nm) into the green (~550 nm) and comprises two distinct band systems. The broader and more extensive double headed band system was readily identified as NS($B\,^2\Pi_{1/2,3/2} \rightarrow X\,^2\Pi_{1/2,3/2}$), and shows the characteristic 1/2–3/2 spin orbit components (A_0 = 90 cm^{-1}). A second much sharper spectral progression is evident in the 200–330 nm region. By comparison of the vibrational term values calculated for these bands and by comparison of the band frequencies with the known electronic states of NS, a single progression originating out of $v'=0$ for NS($H\,^2\Pi_{1/2} \rightarrow X\,^2\Pi_{1/2}$) was identified. We have recently completed a detailed analysis of this system, reporting on the Franck–Condon factors, r centroids, radiative lifetime, and collisional quenching constants of various species with the NS($H\,^2\Pi$) state.[12] As is evident in the spectrum, the 248 nm laser radiation strongly overlaps the $H_{1/2}(0,3)$ transition near 248.41 nm. The large Franck–Condon factor (FCF) calculated for this band[12] (0.1342) and the sharp appearance of the progression suggests that this state is produced via a resonant interaction with the laser radiation.

A Stern–Volmer quenching study of the NS(H) state indicated a collision free radiative lifetime of 87 ± 14 ns and facile quenching by He, CF_4, and N_2, with the latter two gases quenching near gas kinetic rates.[12] Several bands to the blue of the KrF laser spike are not attributable to NS(H) and have been assigned to progressions out of NS($I\,^2\Sigma^+$) and NS($G\,^2\Sigma^+$), although unequivocal assignment of these bands is made difficult by the large number of nested energy states in the 40 000–45 000 cm^{-1} range.[12]

Time profiles of the NS(B) and NS(H) emission were recorded for various He buffer gas pressures. Figure 3 shows the time profile of the NS($B \rightarrow X$) intensity recorded for the 0,4 band near 394.4 nm with no added quencher. The profile reveals a rapid rise of ~30 ns followed by a much slower decay over several microseconds. The lifetime of the decay of 1.1 ± 0.2 μs compares favorably with the known radiative lifetime of NS(B, $v'=0$) of 1.04 ± 0.1 μs,[10] and we associate the decay with radiative and collisional removal of the excited state. The rise was found to track the excimer laser pulse (FWHM pulse time = 17 ns), and was invariant with added quencher. The time history of the NS($H \rightarrow X$) fluorescence was similar, and also indicated a pressure invariant, laser limited rise but with a considerably faster decay rate as noted above, i.e., $\tau_{1/e}$ = 87 ns.[12] Both the NS(H) and NS(B) intensities were found to vary as the third power of the laser flux.

From Fig. 2 it is readily apparent that progressions out of higher v' levels of the B state are obscured due to the strong overlap by the H fluorescence. However, since the B radiative lifetime is considerably longer than the H, the H fluorescence was easily discriminated against by setting a photon counter gate delay equivalent to several H lifetimes, e.g., 625 ns. This gate delay also discriminates against any overlapping transitions from other NS states in this region, namely the NS(G) and NS(I) whose lifetimes are estimated to be ⩽20 ns. The time delayed $B \rightarrow X$ spectrum recorded with the 0.5 m mono/1P28/gated photon counter is shown in Fig. 4. The spectrum, collected for a gate width of 2 μs and for an excimer flux of 70 mJ cm^{-2}, reveals a highly excited nascent vibrational distribution with population in levels up to at least $v'=10$. It is known that NS(B) ceases to fluoresce from vibrational levels above $v'=12$ because of predissociation to N(^4S) + S(^3P).[18] However, population in higher vibrational levels could not be confirmed.

As an aid in measuring the excited vibrational populations and rotational temperatures a spectral simulation code[19] was employed to fit synthetic spectra with the experimentally obtained spectra, and a relevant fit to the NS(B) spectrum is shown in Fig. 4. The vibrational distribution yielding this fit is plotted in Fig. 5 which plots the relative vibrational population against the vibrational term energy. We note that the intensity discrepancies between

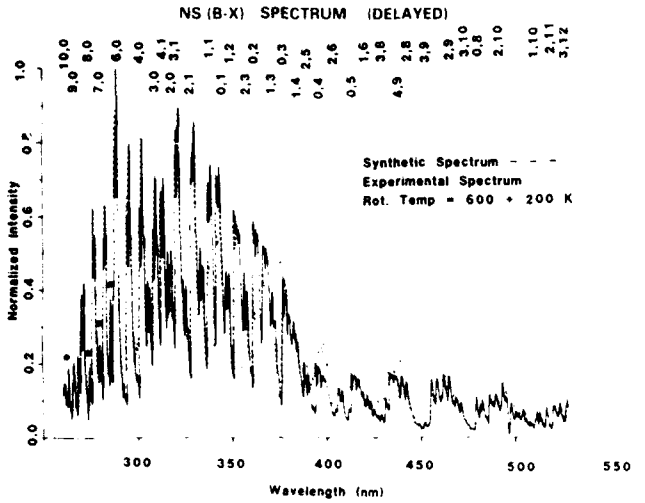

FIG. 4. Time delayed NS($B \rightarrow X$) spectrum with a superimposed synthetic spectrum. The peaks marked with an asterisk do not belong to the NS(B) system and are probably due to emission from higher lying states of NS, eg., $-$NS(H), NS(G), and NS(I).

the synthetic and experimental spectrum in the 390–450 nm region, i.e., notably the (0,4), (1,5), (2,6), (0,5), and (0,6) may be due to photon counter pulse pile up. Consequently, larger uncertainties in the relative populations of the $v'=0$, 1, and 2 levels are indicated in Fig. 5. From Fig. 5 it is evident that the photolysis produces a non-Boltzmann vibrational distribution with large relative populations in high NS(B) v' levels. In contrast to the vibrational excitation, a fairly cool rotational temperature of 600 ± 200 K was calculated. Hence, under these photolysis conditions the nascent NS(B) is generated vibrationally hot yet rotationally cool. Further, an analysis of the rotational temperature for the H state[12] revealed a similarly cool rotational temperature of 330 ± 100 K.

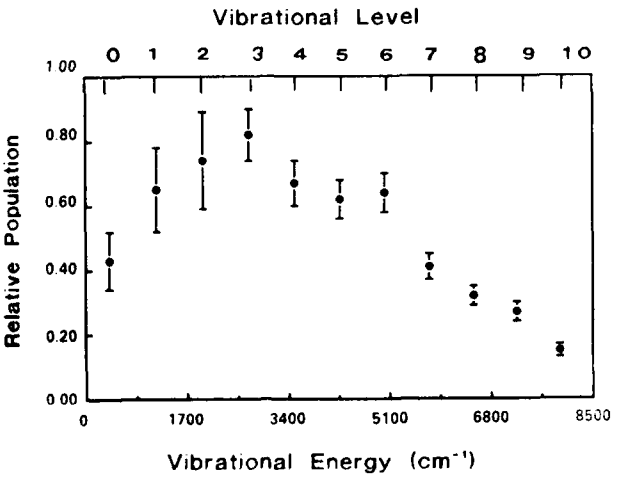

FIG. 5. Nascent NS($B\,^2\Pi$) vibrational population distribution produced from the 248 nm photolysis of S_4N_4. The total pressure in the cell was 0.8 Torr.

Other photolysis products such as sulfur or metastable states of nitrogen were not detected. For example, no prompt emission from N_2^* or S_2^* was detected. Production of the first excited state of nitrogen, $N_2(A\,^3\Sigma^+)$, was tested for by adding a small amount of NO to the photolysis chamber. The presence of $N_2(A)$ would typically be signaled by strong NO γ band emission due to the rapid energy transfer reaction: $N_2(A) + NO(X) \rightarrow N_2(X) + NO(A)$.[20] No γ band emission was detected. From NO(A) detection limits determined in previous flow tube experiments[21] we estimate the $N_2(A)$ density to be $\leqslant 1 \times 10^6$ mol cm^{-3}. The production of $S_2(X)$ was investigated, as described below, by LIF excitation scans on the $S_2(X\,^3\Sigma_g^- \rightarrow B\,^3\Sigma_u^-)$ system.

B. Photolysis at 222 nm

Photolysis of S_4N_4 at 222 nm probes vibronic structure, lying on the wing, to the blue of the primary absorption centered near 250 nm. The absorption cross section at 222 nm is equal to 8.14×10^{-18} cm^2, and while considerably reduced from the 248 nm value is, nonetheless, substantial and provides a further probe of the photodissociation dynamics of the molecule.

Photolysis of 10–20 mTorr of the tetramer at the KrCl wavelength again produced a visible blue fluorescence, albeit much weaker in intensity than that observed in the 248 nm case. Wavelength dispersion of the emission produced a spectrum, similar to that shown in Fig. 3, with two distinct band systems. NS($B \rightarrow X$) emission was again observed in the 270–550 nm region with fluorescence originating from v' levels as high as eight. However, the NS(B) emission intensity generated via 222 nm photolysis was <0.1 of the NS(B) intensity observed during the 248 nm photolysis, for similar conditions of fluence. More strikingly, NS(H) emission was no longer observed in the short wavelength region being replaced with the double banded spectrum shown in Fig. 6(a).

This spectrum is attributable to the NS($C\,^2\Sigma^+ \rightarrow X\,^2\Pi_{1/2,3/2}$) transition and shows only a single progression originating out of $v'=2$. Each band in the spectrum shows two components separated by 221.5 cm^{-1} equivalent to the spin orbit energy splitting of the NS ground state.[22] The short and long wavelength components are due to the 1/2 and 3/2 transitions, respectively.

Temporal histories recorded for the (2,4) and (2,5) transitions with no added diluent gas showed very spiked Gaussian intensity profiles with a FWHM of 17 ns. The profiles were unaffected by addition of Ar up to 9 Torr. From these time histories the NS($C\,^2\Sigma^+$, $v'=2$) fluorescent lifetime is estimated to be $\leqslant 10$ ns. This is consistent with a 6.5 ns radiative lifetime determined by Silvers and Chiu for the NS(C) $v'=0$ level via a Hanle effect measurement.[23] In a more detailed study of the NS(C) state Chiu and Silvers[24] observed absorption, emission, and fluorescence from the $v'=0$, 1, and 2 levels. They noted a weakening of the bands originating from $v'=1$ and 2 relative to that from the $v'=0$ level. They ascribed this diminution in intensity to a weak predissociation in the $v'=1$ and 2 levels,

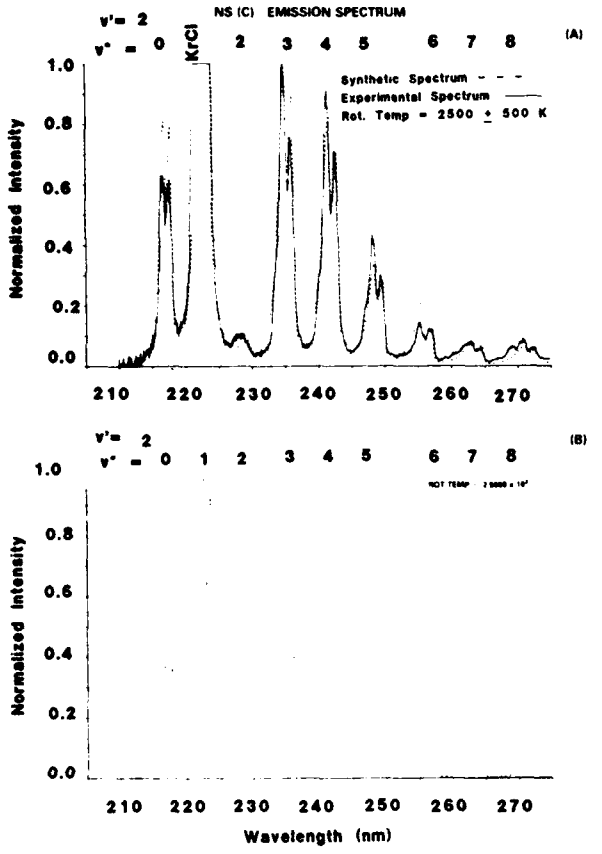

FIG. 6. (a) Emission spectrum collected in the 200–300 nm region for photolysis at 222 nm. The broad band near 222 nm is the KrCl laser spike. (b) Synthetic spectrum of the NS($C\,^2\Sigma^+$, $v'=2$) progression showing the relative magnitude of the (2,1) band.

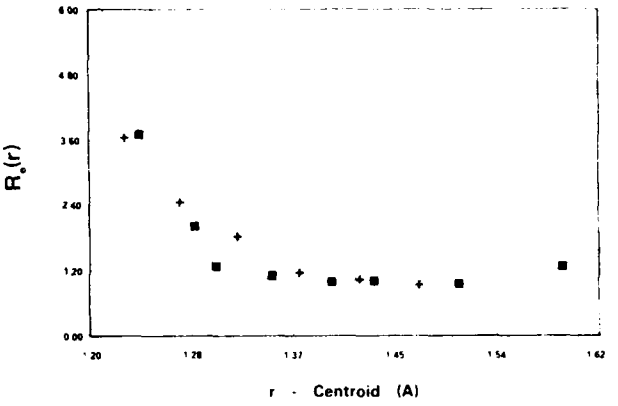

FIG. 7. The apparent dependence of the electronic transition moment on the r-centroid for NS($C\,^2\Sigma^+$, $v'=2$) as given by a plot of $(p_{v',v''}/q_{v',v''})^{1/2}$ vs r. The solid line represents a fourth-order polynomial fit to the data. □—estimated value for the (2,2) band based on $p_{2,2} \approx 1000 - \Sigma p_{v',v''}$, + —Jeffries *et al.* data for NS($C\,^2\Sigma^+$, $v'=0$); this data was not included in the polynomial fit.

an idea supported by configuration interaction calculations on the $C\,^2\Sigma^+$ adiabatic potential well.[25] Hence, the short radiative lifetime we measure for the $v'=2$ level may be due to predissociation.

It is of interest to compare the photolytically induced spectrum in Fig. 7(a) with Chiu and Silver's fluorescence spectrum (their Fig. 3) obtained by exciting the NS(X) produced in an active nitrogen discharge with a deuterium lamp. They observe strong emission out of $v'=0$ and much weaker $v'=1$ and 2 progressions. Moreover, their (2,v'') band intensities are barely discernable from the baseline noise, and only the (2,1), (2,3), and (2,4) are observable. In marked contrast, the photolytically induced spectrum shows no emission from the $v'=0$ and 1 levels and intense emission only from $v'=2$, with this progression extending to at least $v''=8$. This behavior suggests interaction of the 222 nm excimer radiation with an energetically resonant state of NS. From the C spectrum it is clear that the $(2,1)_{1/2}$ and $(2,1)_{3/2}$ bands at 222.46 and 223.56 nm are resonant with the 222 nm laser pulse (FWHM=1 nm), and that excimer laser pumping of these transitions may give rise to the observed spectrum, provided the photodecomposition creates a nascent ground state population which is vibrationally excited, i.e., NS(X, $v''=1$) must be populated. As noted above, in the 248 nm case an analogous LIF process is hypothesized to account for NS(H) fluorescence, i.e., the 248 nm radiation pumps the NS(X, $v''=3$) → NS($H_{1/2}$, $v'=0$) transition at 248.4 nm, thereby requiring nascent population in NS(X, $v''=3$). LIF excitation scans on the NS $X \rightarrow B$ transition, described below, confirm the production of vibrationally excited ground state populated up to at least $v''=4$ in both the 222 and 248 nm photolysis.

A number of experiments were performed in which the relative intensity of the NS C–X emission was recorded as the incident fluence of the 222 nm pulse was varied. The data indicate a quadratic dependence of the NS(C–X) intensity on excimer fluence.

C. Determination of Franck–Condon factors, *R* centroids, and vibrational transition probabilities for the NS($C\,^2\Sigma^+$) state

Due to the enhancement of the NS(C, $v''=2$) emission spectrum relative to others reported to date,[24] a more extensive spectral analysis of the emission was undertaken, with calculations of FCF's, r centroids, vibrational transition probabilities and transition moments. An RKR computer code was employed in calculating the potential function $U(r)$ and classical turning points for both NS(C) and NS(X) using existing Dunham coefficients for each state.[22] FCF's and r centroids were thus obtained for the first three, and only observed, vibrational levels of the C state, and are presented in Table I. These values compare favorably with past values calculated using Morse wave functions.[8,24]

Vibrational transition probabilities ($p_{v',v''}$) were calculated from the relation

$$p_{v',v''} \propto A_{v',v''}(\lambda_{v',v''})^3, \tag{1}$$

where A is the Einstein coefficient for spontaneous emission and is proportional to the intensity of fluorescence in a given vibrational band at wavelength $\lambda_{v',v''}$. Relative

TABLE I. RKR Franck–Condon factors and r centroids for NS($C\,^2\Sigma^+$).

Transition	$(q^{1/2}+q^{3/2})/2$[a]	$(r^{1/2}+r^{3/2})/2$
0,0	612	1.474
0,1	280	1.425
0,2	80	1.379
0,3	18	1.335
0,4	3.8	1.296
0,5	0.64	1.257
0,6	0.11	1.215
1,0	311	1.530
1,1	161	1.485
1,2	301	1.432
1,3	158	1.388
1,4	50	1.342
1,5	14	1.303
1,6	3.2	1.270
1,7	0.65	1.220
2,0	68	1.590
2,1	382	1.539
2,2	18	1.505
2,3	202	1.435
2,4	200	1.400
2,5	88	1.350
2,6	31	1.304
2,7	9	1.287
2,8	2	1.242

[a]Values multiplied by 1000.

$A_{v',v''}$ were obtained from area integration of the discreet v',v'' spectral bands taken from the 0.25 m polychromator/diode array response corrected spectrum shown in Fig. 6(a) [excluding the (2,1) band]. Using the known $\lambda_{v',v''}$[22] Eq. (1) was used to calculate relative $p_{v',v''}$ for the $v'=2$ progression. The results, presented in Table II, are compared with the RKR computed Franck–Condon factors ($q_{v',v''}$), and indicate a gradual increase in $p_{v',v''}$ over $q_{v',v''}$ with increasing v''. This implies a variation of the electronic transition moment $[R_e(r_{v',v''})]$ with internuclear separation. The r centroid relation,[26]

$$p_{v',v''}=[R_e(r_{v',v''})]^2 q_{v',v''}, \tag{2}$$

TABLE II. Comparison of NS($C\,^2\Sigma^+$, $v'=2$) vibrational transition probabilities with the RKR Computed Franck–Condon factors.

$v'=2$, $v''=$	$(q^{1/2}+q^{3/2})/2$[a]	p^{exp}
0	68	109
1	382	(254)[b]
2	18	16
3	202	202[c]
4	200	194
5	88	107
6	31	50
7	9	36
8	2	30

[a]p and q values multiplied by 10^3.
[b]The $p_{2,1}$ value was estimated from: $p_{2,1} \simeq 1000 - \Sigma\, p_{v',v''}$.
[c]The $p_{2,3}$ value is normalized to the $q_{2,3}$ value.

was used to quantify this variation. Figure 7 plots the electronic moment as $(p_{v',v''}/q_{v',v''})^{1/2}$ vs r centroid. According to the RKR calculations, the r centroid varies from 1.24 Å for the (2,8) band to 1.59 Å for the (2,0). Over this interval a smooth decrease in $R_e(r_{v',v''})$ is readily apparent. A similar variation was noted by Jeffries *et al.*[8] in their LIF spectroscopic study of the NS(C, $v'=0$) state, and we have included their data for comparison in Fig. 7. A fourth order polynomial fit to the averaged 1/2 plus 3/2 data yielded the following expression:

$$R_e(r_{v',v''})=\text{const}[1-2.76\,r+2.86\,r^2-1.31\,r^3 +0.226\,r^4 \tag{3}$$

and gives the variation of the transition moment for the region sampled: 1.2 Å $\leqslant r_{v',v''} \leqslant$ 1.6 Å.

Introducing the functional form for $R_e(r_{v',v''})$ given by Eq. (3), and using the RKR calculated $q_{v',v''}$ (see Table I) in the spectral simulation code a best fit NS(C) spectrum was computed and is graphically overlaid on the experimental spectrum. The simulation correctly predicts the (2,2) vibrational node and fits the higher v'' bands correctly in accord with the increasing $R_e(r_{v',v''})$ in this region. Based on the width of the vibronic bands a rotational temperature of 2500 ± 500 K was determined. Since the (2,1) band should have considerable intensity [i.e., $q_{(2,1)}$ = 0.382), and since this band is spectrally obscured by the 222 nm laser light a synthetic spectrum of the entire $v'=2$ progression is presented in Fig. 6(b). This spectrum indicates the relative magnitude of the (2,1) band.

D. NS($X\,^2\Pi$ – $B\,^2\Pi$) LIF excitation scans for 248 nm photolysis

The operation of photolytic channels which produce rotationally and vibrationally excited NS(X) was probed by searching for LIF from NS fragments. Excitation spectra were recorded by monitoring NS($B\rightarrow X$) emission through bandpass filters. Two separate wavelength regions were scanned: 300–310 nm and 360–372 nm using Rh 640 and LDS 750 dyes, respectively. These experiments clearly showed that rotationally and vibrationally excited NS(X) is produced by the 248 nm photolysis as indicated by the LIF spectra shown in Figs. 8 and 13. All of the spectra were corrected for the wavelength dependence of the PDL/filter/PMT combination. As mentioned previously, the minimum excimer pulse to PDL pulse delay time was limited to 2 μs due to the prompt NS(B) fluorescence. No NS LIF was observable with the PDL probe pulse alone.

As a potential photolytic product, the presence of diatomic sulfur was tested by scanning for LIF on the $S_2(X\,^3\Sigma_g^- \rightarrow B\,^3\Sigma_u^-)$ transition. Two wavelength regions were examined: 300–310 nm and 360–370 nm. Since the lifetime of $S_2(B)$ (37 ns) is considerably shorter than NS(B) the NS(B) fluorescence was discriminated against by setting a small gate delay with a gate width equivalent to several $S_2(B)$ lifetimes, i.e., 100 ns. Further, several of these experiments were carried out with high PDL fluences (laser induced pumping rates $\geqslant 1\times10^{10}$ s^{-1}) in order to saturate the S_2 transitions. Under these experimental con-

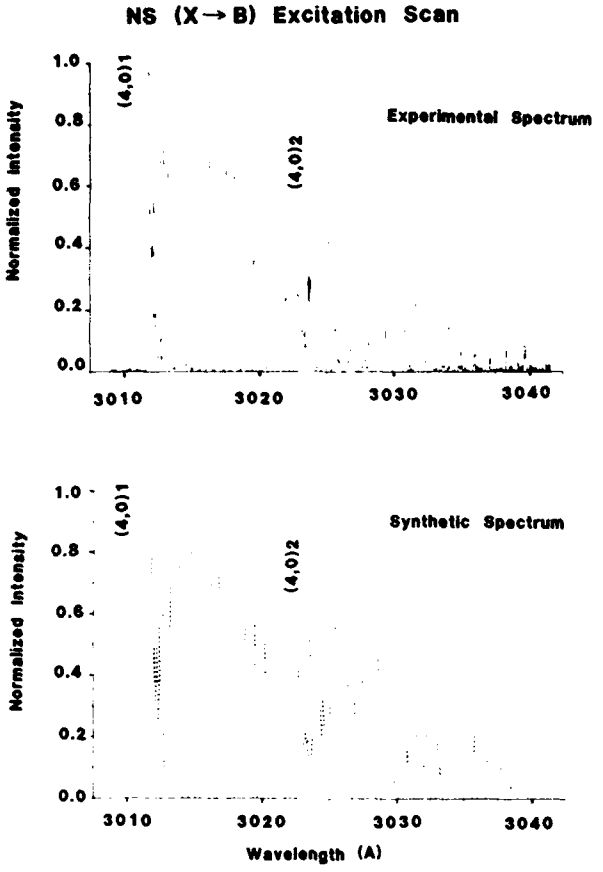

FIG. 8. Experimental (Expt) and simulated (Sim) *LIF* excitation spectra of the (4,0) transition of the $B\,^2\Pi_{1/2,3/2}$–$X\,^2\Pi_{1/2,3/2}$ system of NS produced via the photolysis of S_4N_4 at 248 nm. 1 and 2 designate the 1/2 and 3/2 spin–orbit components, respectively. The total pressure in the photolysis cell was 0.8 Torr, and the probe dye laser delay time was 70 μs.

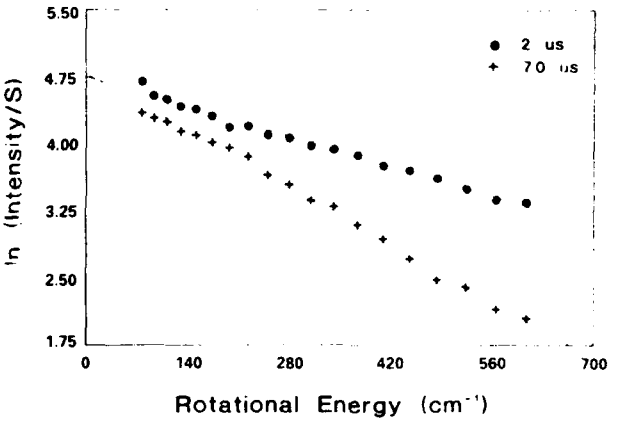

FIG. 9. Quantum state distribution of NS($v''=0$) as measured from (4,0) excitation spectra collected at photolysis to probe pulse delay intervals of 2 and 70 μs, respectively. The latter spectrum is shown in Fig. 8.

ditions no $S_2(B \rightarrow X)$ fluorescence was detected. Based on a two level model for near saturated fluorescence in diatomic molecules[27] we calculate a $S_2(X\,^3\Sigma_g^-)$ detection limit, for our experimental conditions, of 1×10^9 mol cm^{-3}.

E. Internal energy distribution of the NS(*X*) fragments

Since the linewidth of the probe laser (0.01 nm) was not sufficient to fully resolve the individual rotational lines of the NS LIF spectra, the spectral simulation code was modified and was used as an aid in determining vibrational and rotational population distributions. The simulation employed a Gaussian line shape function, a laser line width parameter and the following equation for rotational line intensities:

$$I = kq_{v',v''}\nu_{v',v''}S_{N',N''}P_{v''}Q^{-1}\exp\{-B''N''(N''+1)/kT\}, \quad (4)$$

where k is a proportionality constant, q is a Franck–Condon factor, $\nu_{v',v''}$ is the transition frequency, $S_{N',N''}$ is the Hönl–London factor appropriate to a $\Delta\Lambda=0$ transition, $P_{v''}$ is the population of the v'' vibrational level, Q is the partition function, B'' is the rotational constant, and T is the rotational temperature. Equation (4) is applicable to a Boltzmann rotational distribution. An excitation scan for the (4,0) band of the B–X system is presented in Fig. 8. The appearance is typical for an unperturbed band of this parallel transition, and should show an R branch head, a red degraded P branch, and no Q branch. However, due to the limited laser resolution the P and R branches remain unresolved. The spectrum collected after a 70 μs delay appears thermalized ($N''_{max}=31.5$), and is, indeed, well fit by a spectral simulation utilizing a 340 K rotational temperature. A excitation spectrum recorded for a shorter photolysis to probe pulse delay interval (2 μs) showed a much flatter and broader rotational distribution with a much less distinct R branch head and population in higher N'' ($N''_{max}=58.5$), behavior consistent with a more highly excited rotational population in the ground state. A synthetic fit to this spectrum indicated a rotational temperature of 800±200 K. These "best fit" T_R's are in close agreement with the T_R values calculated directly from the observed (response corrected) spectra. This is indicated in Fig. 9, which plots $\log(I/S_{N',N''})$ vs $-B''N''(N''+1)$ for the (4,0) excitation scans described above. The plots are quite linear, indicative of a Boltzmann distribution in this region. From the slopes of the lines rotational temperatures of 800 and 350 K were determined for the 2 and 70 μs delay times, respectively.

Rotational relaxation was evident as the pump to probe delay time was increased. This is shown in Fig. 10, which plots the rotational temperature of the $(4,0)_{1/2}$ band vs number of collisions with the helium bath gas for low fluence ($F \leqslant 10$ mJ cm^{-2}) photolysis. Evidently, NS(X, $v=0$) is formed with a near nascent rotational temperature of 800±200 K, and a few hundred collisions are required to thermalize the distribution.

The variation in the $(4,0)_{1/2}$ LIF intensity as a function of laser fluence was recorded for conditions of both high and low laser fluence. For these measurements the photolysis to probe pulse delay was set to 20 μs, sufficient

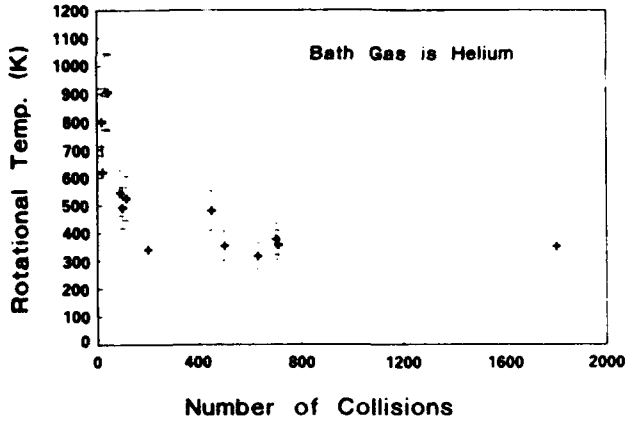

FIG. 10. Collisional cooling of NS(X, $v''=0$, N'') for low fluence photolysis conditions. +—248 nm photolysis, Δ—222 nm photolysis.

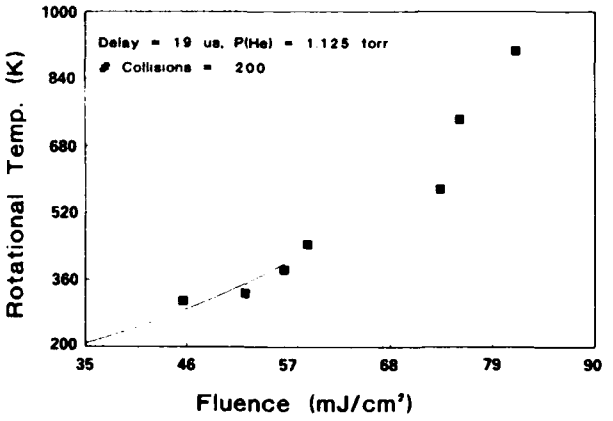

FIG. 12. Variation of the NS(X, $v''=0$) rotational temperature with KrF laser fluence. The solid line represents an exponential fit, of the form $y = a_0 \exp(a_1 x)$, to the data.

time to allow for the relaxation of the rotational manifold. In the low fluence regime ($0.8-25$ mJ/cm^2) the rotational distributions were indeed thermalized. Figure 11 shows a log–log plot of the integrated fluorescent intensity vs excimer laser fluence for the low fluence photolysis. A least squares fit to the data yielded a slope of 2.0 ± 0.2. This quadratic dependence indicates that 2 KrF photons are required to generate an NS(X) photofragment. For the high fluence measurements the rotational distributions did not appear relaxed, and a substantial variation in the rotational quantum state distribution was evident as the laser flux was varied. This effect is quantified in Fig. 12, which graphs the rotational temperature of the $(4,0)_{1/2}$ band vs laser fluence. It is apparent that under high fluence conditions the rotational distribution is much more excited than would be predicted for a quenched distribution. A nearly exponential decrease in rotational temperature with fluence is seen, and as the fluence is reduced the temperature approaches the thermal limit (near 340 K). This behavior is suggestive of a fluence dependent rotational excitation process in the gas medium.

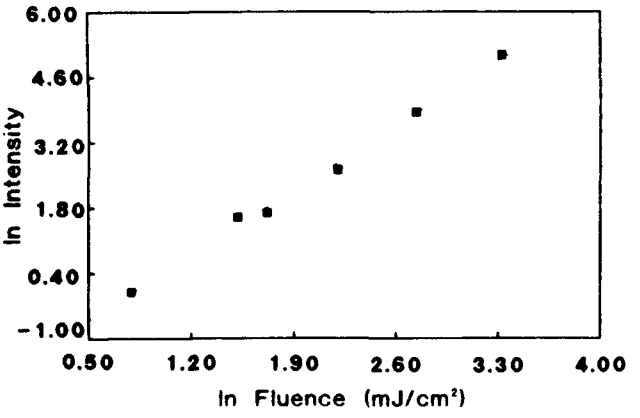

FIG. 11. A plot of the log of the integrated emission intensity of the NS$(4,0)_{1/2}$ band vs log of the KrF laser fluence. The slope of 2.0 ± 0.2 indicates two photons are required to generate the NS ground state.

The variation in the LIF intensity of the $(0,2)_{1/2}$ band was also recorded as a function of laser fluence. In this experiment the delay separating photolysis to probe pulse was set to 70 μs, and the KrF fluence was varied in the range 3 to 17 mJ cm^{-2}. The results, for this higher vibrational level, also indicated a quadratic dependence of intensity with fluence.

Population in vibrational levels above $v''=0$ was probed by scanning the 360–372 nm region. Figure 13 displays a typical LIF excitation scan of this region, collected for a delay interval of 70 μs and at a total pressure of 1.2 Torr. Under these experimental conditions the rotational distribution is equilibrated (i.e., $T_{\rm rot} = 340$ K) while the vibrational distribution remains unperturbed. Hence, the spectral simulation designed to determine relative $P_{v''}$ was simplified as only a single rotational temperature in Eq. (4) needed to be specified.

The rate constant for quenching vibrationally excited NS(X) by He has not been reported. However, we note that excitation spectra collected under low collision conditions ($\sim$30 collisions) and under high collision conditions ($\sim$1300 collisions) showed no significant differences in the vibrational distribution. This indicates the NS(X)–He VET is not a facile process.

Population in the $v''=2$, 3, and 4 levels is evident in the spectrum of Fig. 13(a). Population in $v''=4$ is indicated by the presence of the weak (3,4) bandhead near 361 nm. The spectral code was used in determining the relative vibrational populations in the 2, 3, and 4 levels and an optimized fit is shown in Fig. 13(b). The fractional vibrational populations obtained in this manner are 0.89, 0.07, and 0.03 for $v''=2$, $v''=3$, and $v''=4$, respectively. This distribution was found to be independent of laser fluence. The fit was such that changing $P_{v''=4}$ from 0.03 to 0 removed the (3,4) bandhead, in clear disagreement with the experimental data. Population in higher v'' levels was not evident. The region of the $(5,6)_{1/2}$ band in the vicinity of 371.0 nm was scanned. The FCF for this band is equivalent to the (0,2) transition, with strong LIF signals from the latter being observed. However, no LIF signals were de-

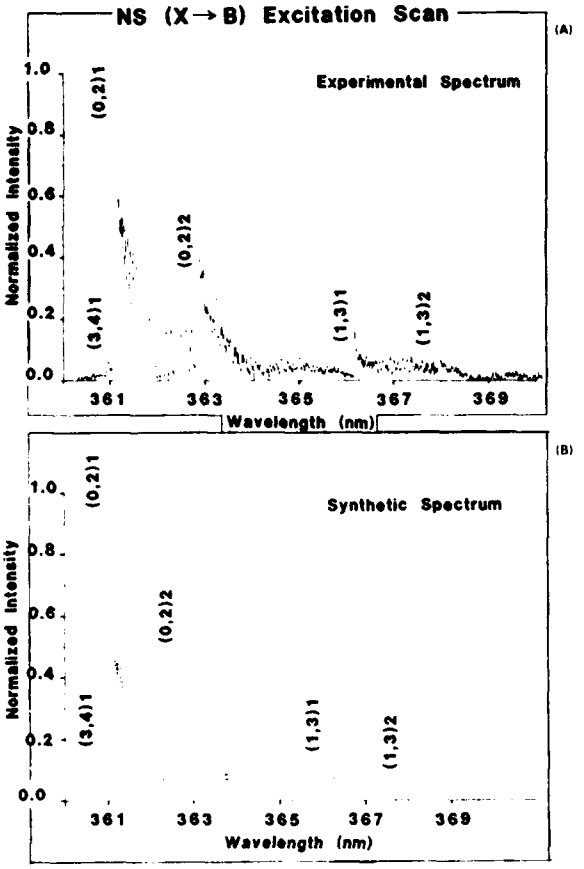

FIG. 13. Experimental (a) and synthetic (b) NS ($X \rightarrow B$) LIF excitation spectra showing population in $v'' = 2$, $v'' = 3$, and $v'' = 4$ vibration levels.

tected in this region even with substantially higher pressures of S_4N_4 in the photolysis cell. From determinations of signal to noise ratios, i.e., $-2S/N$ in the LIF scans we estimate $P_{v''=6} \leqslant 0.01$.

IV. DISCUSSION

The photolytic process at 248 nm leading to the formation of NS(B) and NS(H) is complicated by the variety of $(SN)_x$ intermediates which may be formed, and by the energetics of these species. However, in view of the data, presented above, it appears that the NS(B) and NS(H) are formed from different precursor species. For example, the emission spectrum (Fig. 4) indicates the nascent NS(B) is produced vibrationally hot, in a non-Boltzmann distribution with v' levels as high as ten populated. The NS(B) is also formed with some degree of rotational excitation as $T_{\text{rot}} = 600 \pm 200$ K. In contrast, the NS(H) appears rotationally cold, and the collected emission is reminiscent of a fluorescence scan with only a single vibrational level ($v' = 0$) emitting. Additional considerations, as previously noted, such as the energy overlap of the $H(0,3)$ transition with the KrF frequency, the population detected in ground state vibrational levels, and the disappearance of the H fluorescence when the excimer wavelength is changed clearly indicates the H state is formed by laser excitation of vibrationally excited ground state NS fragments. Since the KrF wavelength is above the dissociation limit for NS(B), the B fluorescence cannot arise from an analogous KrF excitation of NS(X) molecules. Rather, some higher order $(SN)_x$ homolog must be the precursor to NS(B). We further note that the temporal history of the B emission indicates that the NS(B) is not generated via a collisional process. Rather, its production appears photolytically induced. The fluence data indicates that NS(B), as well as the more energetic NS(H), is formed in a three photon process. Aside from the prompt NS(B) and NS(H) emissions, the excitation scans reveal that rotationally and vibrationally excited NS(X) is also a product of the photolysis, and is produced in a two photon event. In light of these considerations, the following general mechanism is proposed to qualitatively account for the NS(B), NS(H), and NS(X,v) states produced in the KrF photolysis of S_4N_4:

$$c\text{-}S_4N_4 + 2h\nu \rightarrow a\text{-}S_3N_3 + \text{NS}(X,v),$$

$$\Delta H = -132 \text{ kcal mol}^{-1}, \quad \text{(R1)}$$

$$a\text{-}S_3N_3 + h\nu \rightarrow \text{NS}(B,v) + c\text{-}S_2N_2,$$

$$\Delta H = -21 \text{ kcal mol}^{-1}, \quad \text{(R2)}$$

$$\text{NS}(X,v''=3) + h\nu \rightarrow \text{NS}(H,v'=0), \quad \text{(R3)}$$

where reaction (R3) shows the resonant excitation which produces the NS(H) state, and where c and a represent the cyclic and acyclic isomers, respectively. The heats of reaction have been calculated from $\Delta H_f(S_xN_y)$ values previously determined via a MOPAC calculation.[28]

Reaction (R1) depicts a multiphoton excitation of cyclic S_4N_4 to an excited singlet state which subsequently dissociates yielding vibrationally excited NS(X) fragments and an acyclic S_3N_3 fragment. The large value of the exothermicity for this process is not surprising, considering the 2 uv photon excitation contributes 230 kcal mol^{-1} at the 248 nm wavelength. The heat of reaction is sufficient to provide for the vibrational excitation of the NS(X) fragment ($v'' = 4$ requires 13.5 kcal), and for a large remnant energy balance of over 100 kcal mol^{-1}. For comparison, a one photon excitation would be much less exothermic (-17 kcal mol^{-1}) and would be nearly thermal neutral when the vibrational energy in the NS fragment is accounted for. That two photons are required to reach the dissociative state is also supported by the results of MO calculations on c-S_4N_4, as described below.

If the partitioning of excess energy between the NS(X) and S_3N_3 photofragments in reaction one is statistical in nature, the more massive S_3N_3 fragment, with 12 vibrational modes, would consume the majority of the vibronic energy. Further, provided the excited S_4N_4 electronic state, from which dissociation occurs, has approximately the same S–N geometry as the S_4N_4 ground state, the energy available to the NS fragment would not be expected to exceed that available from simple geometric relaxation of the NS bond length in c-S_4N_4. The energy available in contracting the N–S bond length in c-S_4N_4 (1.63 Å)[13] to its equilibrium value in monomeric NS (1.495 Å)[22] is

readily obtained from the RKR potential well of the NS ground state. We calculate that 8.6 kcal mol^{-1} of vibrational energy can be imparted to the released NS(X) fragment. This represents enough energy to populate NS(X) up to $v''=3$. This result agrees reasonably well with the experimental measurements which showed small relative populations of 0.07 and 0.03 in the $v''=3$ and $v''=4$ levels, respectively, and no measurable population in higher levels. Thus, it appears that the excited state is sufficiently long lived (on the order of a few vibrational periods) to allow for, at least, partial vibrational energy randomization in the transitional S_4N_4 structure.

Evidently, from the rotational excitation observed in the NS(X, $v=0$) fragment, a relatively small fraction of the excess energy available in the primary photodissociation ends up in NS rotation. Rotational energies much higher than 1000 cm^{-1} (2.9 kcal) were not detected. Intuitively, the presence of some rotational excitation in the NS photofragments indicates that the dissociation is not linear, and that there is some excitation of the bending modes in the transition.

The photofragments produced in reaction one may undergo secondary photolytic processes, as indicated by reactions (R2) and (R3). Reaction (R2) shows the NS(B) being formed from the single photon excitation/dissociation of an a-S_3N_3 intermediate. The observation of NS(B, $v_{max}=10$) places an energy constraint on reaction (R2), and we are required to choose the cyclic form of S_2N_2 over the acyclic form, since the latter would lead to $a+23$ kcal mol^{-1} endothermic process. The reaction exothermicity thus calculated (-21 kcal mol^{-1}) is, considering the error of the MOPAC[28] calculation, just sufficient to populate NS up to its observed vibrational maximum. Thus, it would appear that the reaction exothermicity is completely consumed in NS(B) vibration. Since it is reasonable to assume that some energy is partitioned to NS(B) translation and S_2N_2 vibration–translation, the ΔH for reaction (R2) is likely to be < -21 kcal mol. This would require a larger energy content, than determined by the MOPAC calculation, for the a-S_3N_3 precursor. As explained above, the a-S_3N_3 molecules are likely to be formed with considerable internal excitation.

Other S_4N_4 photodecomposition mechanisms may certainly be written. However, the majority of these can be ruled out based on considerations of energetics and the experimental data. For example, a mechanism involving the nonlinear absorption of three photons by the tetramer to produce NS(B) and NS(H),

$$c\text{-}S_4N_4 + 3h\nu_{248} \rightarrow NS(B) + NS(H) + S_2N_2, \qquad (R4)$$

is endothermic by 37 kcal mol^{-1}, and does not account for the specific NS(H, $v'=0$) fluorescence or the two photons required to produce the ground state.

The data for the KrCl photolysis is qualitatively similar to that obtained in the KrF photolysis. For example, the 222 nm emission spectrum indicates formation of vibrationally hot NS(B), the LIF scans show that rotationally and vibrationally excited ground state NS photofragments are produced, and the NS(C) emission indicates a resonant excitation by the laser on an NS(X–C) transition. Further, the time histories of the emissions suggest the NS(B) and NS(C) formation rates are photolytically driven and are independent of collisional processes. Given these similarities an analogous mechanism is proposed for the photodissociation at 222 nm:

$$c\text{-}S_4N_4 + h\nu_{222} \rightarrow NS(X,v) + a\text{-}S_3N_3, \quad \Delta H = -32 \text{ kcal mol}^{-1}, \qquad (R5)$$

$$a\text{-}S_3N_3 + h\nu_{222} \rightarrow NS(B,v) + c\text{-}S_2N_2, \quad \Delta H = -35 \text{ kcal mol}^{-1}, \qquad (R6)$$

$$NS(X,v''=1) + h\nu_{222} \rightarrow NS(C,v'=2), \qquad (R7)$$

where the linear dissociation of the tetramer [reaction (R5)] is supported by the quadratic dependence of the NS(C) fluorescence intensity on KrCl excimer fluence. The energy release for reactions (R5) and (R6) is high enough to account for the observed NS(X) and NS(B) vibrational excitation, i.e., NS(X, $v=4$) requires 13.5 kcal mol^{-1} and NS(B, $v=8$) requires 17.5 kcal mol^{-1}. The observation of NS(B, $v_{max}=8$) again restricts the choice of the S_2N_2 photofragment to the cyclic form.

The strong variation in T_{rot} with KrF fluence that is depicted in Fig. 12 suggests the operation of a fluence dependent, rotational excitation process in the photolysis zone. A second order process involving an efficient $V \rightarrow R$ energy transfer could account for the observed behavior. Due to the large absorption cross section of S_4N_4 at 248 nm large densities of NS(X, v'') and $S_3N_3(v)$ may be produced from the primary photolysis step [reaction (R1)]. These species could react further in energy transfer processes

$$NS(v) + NS(v,N) \rightarrow NS(v-1) + NS(v,N+nJ) + \Delta E, \qquad (R8)$$

$$S_3N_3(v) + NS(v,N) \rightarrow S_3N_3(v-1) + NS(v,N+nJ) + \Delta E, \qquad (R9)$$

where nJ indicates n additional rotational quanta. The densities of vibrationally excited photofragments will depend on laser fluence. For high fluence photolysis ($F \geqslant 75$ mJ cm^{-2}) the calculated dissociation is near unity.[29] If we assume the V–R transfer has a ~ 20 μs lifetime, i.e., the rotational excitation process was observed at a 20 μs delay, and that the high fluence photolysis of 10 mTorr S_4N_4 produces $\sim 1 \times 10^{15}$ mol cm^{-3} of NS(v) + $N_xS_y(v)$ photofragments then the calculated second order rate constant $k_{V-T} \simeq 10^{-11}$ cm^3 s^{-1}. This V–R rate coefficient is not untypical of those reported by Moore for a large class of polyatomics.[30]

Molecular orbital calculations, both semiempirical[31] and *ab initio*,[32] indicate the S_4N_4 ground state to be a singlet, and specify the intense 250 nm absorption band as the molecules highest occupied molecular orbital–lowest unoccupied molecular orbital (HOMO–LUMO) transition; giving it a $B_2 \rightarrow E$ designation. The LUMO is a degenerate Π orbital and is antibonding, with respect to the S–S linkage. The *ab initio* calculations indicate that the B_2–E energy separation is 224 kcal mol^{-1}, and that there are four,

nearly resonant, energy states (designated by *) situated 230 kcal above the E level (LUMO). Since these calculations have not incorporated electron correlation, the energy separations are clearly too large ($\sim 2x$); this may be seen by comparing the measured B_2–E ΔE of 120 kcal mol^{-1} (obtained from the 250 nm spectral feature shown in Fig. 1) with the calculated B_2–E ΔE value of 224 kcal mol^{-1}. Applying a correction factor of $\times 0.5$ to the calculated values yields a B_2 to * state ΔE of 227 kcal mol^{-1}, which is in good agreement with the fluence and thermochemical data indicating that two 248 nm photons (230 kcal) are required to reach the dissociative state. The calculations suggest that a two photon absorption by S_4N_4 is a resonant process (sequential excitation) in which the first photon promotes an electron to the E antibonding Π orbital (perhaps with rupture of the weak S linkage), and the absorption of a second photon promotes the electron from the E state to one of the four upper * states. It is likely that the * states are repulsive or very weakly bound, and rapidly dissociate to yield a nonlinear a–S_4N_4 intermediate. The temporal histories of the emissions indicate that the lifetimes of these states is $\tau \ll 30$ ns.

V. SUMMARY AND CONCLUSIONS

Emission from several electronically excited states of NS is observed when the energetic molecule S_4N_4 is photolyzed with radiation from an excimer laser. Photolysis at 248 nm generates fluorescence from the $B(^2\Pi_{1/2,3/2})$, $H\,^2\Pi_{1/2}$, $G\,^2\Sigma^-$, and $I\,^2\Sigma^-$ states of NS. NS($B\,^2\Pi_{1/2,3/2}$) and NS($C\,^2\Sigma^-$) fluorescence is observed when the photolysis wavelength is changed to 222 nm. The NS(H) and NS(C) spectra are postulated to arise from a resonant interaction between the KrF and KrCl excimer photons, respectively, and vibrationally hot ground state NS. LIF excitation scans confirm the production of rotationally and vibrationally excited NS(X) up to $v=4$. An analogous mechanism is thought to generate some of the $v'=2$ bands of NS(I,G).[12]

The experimental data, thermochemistry, and *ab initio* calculations on the tetramer support a nonlinear (two photon) dissociation step for parent S_4N_4 at the 248 nm wavelength. It is postulated that the dissociation produces vibrationally excited NS and an acyclic S_3N_3 photofragment. The observation of the maximum vibration in NS(X), i.e., $v''=4$ is consistent with statistical energy partitioning in the photofragments and suggests the a–S_3N_3 segment is formed with considerable internal excitation. The data indicates the a–S_3N_3 fragment may undergo further photodissociation leading to the production of vibrationally hot NS(B) and an S_2N_2 molecule, and that these dissociations occur on a time scale much shorter than the laser pulse. Surprisingly, no evidence for the formation of sulfur or nitrogen was obtained. This may be contrasted with the explosive or thermal decomposition mechanisms which are known to generate both nitrogen and sulfur.[33,34]

The short radiative lifetime measured for the NS(C, $v'=2$) state ($\tau \leqslant 10$ ns) may be indicative of some predissociation in this vibration. The NS(C) intensity distribution and the calculated FCF's are used to evaluate the C states electronic transition moment variation with internuclear separation; a small dependence was found with R_e increasing with decreasing r.

The photolysis of S_4N_4 at excimer wavelengths may be used as an alternate method for producing the NS radical for kinetic and spectroscopic study. In comparison to the standard method for NS production (reaction of active nitrogen plus sulfur compound) the photolysis is largely free from interferences, i.e., S_2, N_2, and creates a relatively high distribution of vibrationally excited ground state. The latter effectively red shifts the absorption spectrum of NS such that NS electronic states with energies in excess of 43 000 cm^{-1} are more readily accessed via optical excitation.

ACKNOWLEDGMENTS

The authors express their appreciation to Dr. Gilbert Mains for his work on the *ab initio* M. O. calculations on S_4N_4. We also express our thanks to Dr. Robert Coombe, which two of the authors (A.P.O. and T.L.H.) know as scientific mentor and friend, for helpful discussions relating to this work, as well as past works.

[1] J. B. Jeffries and D. R. Crosley, Combust. Flame **64**, 55 (1986).
[2] C. A. Gottlieb, J. A. Ball, E. W. Gottlieb, C. J. Lada, and H. Penfield, Astrophys. J **200**, L147 (1975).
[3] T. B. H. Kuiper, B. Zuckerman, R. K. Kakar, and E. N. R. Kuiper, Astrophys. J **200**, L151 (1975).
[4] T. L. Henshaw and A. P. Ongstad, *Investigation of* NS($B^2\Pi$) *as the Optically Active Medium for a Short Wavelength Chemical Laser* (1989), unpublished report.
[5] D. G. Sutton and S. N. Suchard, Appl. Opt. **14**, 1898 (1975).
[6] K. Raghuveer and N. A. Narasimham, J. Astrophys. Astron. **3**, 13 (1982).
[7] H. Obase, I. Nagano, M. Tsuji, and M Nishimura, J. Phys. Chem. **89**, 257 (1988).
[8] J. B. Jeffries, D. R. Crosley, and G. P. Smith, J. Phys. Chem. **93**, 1082 (1989).
[9] A. Jenouvier and B. Pascat, Can. J. Phys. **58**, 1275 (1980).
[10] J. B. Jeffries and D. R. Crosley, J. Chem. Phys. **86**, 6839 (1987).
[11] I. J. Wysong, J. B. Jeffries, and D. R. Crosley, J. Chem. Phys. **91**, 5343 (1989).
[12] T. H. Henshaw, A. P. Ongstad, and R. L. Lawconnell, J. Chem. Phys. **96**, 53 (1992).
[13] Tetrasulfur tetranitride (S_4N_4) is in the form of an eight-membered ring of alternating N and S atoms. The N–S bond distances are all equivalent at 1.63 A, which lies between the value for a NS single bond (1.74 A) and that for an NS double bond (1.54 A). In a similar manner, the distance between the two trans sulfur atoms (2.58 A) is substantially shorter than the sum of the van der Waals radii (3.7 A) and somewhat longer than a S–S single bond (2.08 A). This implies weak S–S bonding an idea supported by molecular orbital calculations (Ref. 31). It is believed that it is this weak bonding between the sulfur atoms that causes the molecule to pucker into its characteristic tub or boat configuration. The NS bond order of 1.5 is most plausibly explained by a π electron system, which is due to p_π(nitrogen)–d_π(sulfur) overlapping. See H. G. Heal, in *Inorganic Sulfur Chemistry*, edited by G. Nickless (Elsevier, Amsterdam, 1968); O. Glemser, Angew. Chem. Intern. Edit. **2**, 530 (1963).
[14] C. K. Barker, A. W. Cordes, and J. L. Margrave, J. Phys. Chem. **69**, 334 (1965).
[15] M. Villena-Blanco and W. L. Jolly, Inorg. Synth. **9**, 98 (1967).
[16] J. Mason, J. Chem. Soc. A, 1567 (1969).
[17] P. S. Braterman, J. Chem. Soc. 2297 (1965).
[18] Y. Matsumi, T. Munakata, and T. Kasuya, J. Phys. Chem. **88**, 264 (1984).

[19] R. I. Lawconnell, *NS(B) Spectrum Theory and Code*, FJSRL TR-89-0005, USAFA, CO 80840, 1989.
[20] W. G. Clark and D. W. Setser, J. Phys. Chem. **84**, 2225 (1980).
[21] A. P. Ongstad, T. L. Henshaw, R. I. Lawconnell, and W. G. Thorpe, J. Phys. Chem. **94**, 6724 (1989).
[22] K. P. Huber and G. Herzberg, *Constants of Diatomic Molecules* (Van Nostrand, New York, 1979).
[23] S. J. Silvers and C. Chiu, J. Chem. Phys. **61**, 1475 (1974).
[24] C. Chiu and S. J. Silvers, J. Chem. Phys. **63**, 1095 (1975).
[25] G. C. Lie, S. D. Peyerimhoff, and R. J. Buenker, J. Chem. Phys. **82**, 2672 (1985).
[26] P. A. Fraser, Can. J. Phys. **32**, 315 (1954).
[27] Assuming a two level system, in steady state, and near saturation [see A. P. Baronavski and J. R. McDonald, Appl. Opt. **16**, 1897 (1977)] and R. P. Lucht in *Laser Spectroscopy and its Applications*, edited by L. J. Radziemski, R. W. Solarz, and J. A. Paisner (Marcel Dekker, New York, 1987), the detection limit may be calculated from $N_1^0 = \{4\pi\eta_p/(A\ Vc\ \epsilon\ \Omega\ \Delta t)\} \times \{[Q + A + (B_{12} + B_{21})I_\nu]/B_{12}\}\ I_\nu$, where N_1^0 is the lower state number density of the unperturbed system, η_p is the number of photons (incident on the photocathode) required to generate 1 photoelectron, A and B are Einstein coefficients for levels 1 and 2, Vc is the fluorescence probe volume, ϵ is the efficiency of the optical collection system, Ω is the solid angle subtended by the collection optics, Δt is the laser pulse time, Q is the total upper level quenching rate, and I is the laser intensity. The calculation was done for the (6,0), $R(20)$ line for saturable pumping, i.e., $(B_{12} + B_{21})I_\nu \gg Q + A$, and used the following values: $\eta_p = 6.5$ (15% quantum efficiency), $A = 2.7 \times 10^7\ s^{-1}$, $V_c = 0.016\ cm^3$, $\Delta t = 1 \times 10^{-8}$ s, $\epsilon = 0.1$, and $\Omega = 0.012$ sr.
[28] MOPAC (see J. J. P. Stewart, MOPAC Manual (6th ed.), *A General Molecular Orbital Package*, FJSRL TR-88-0007, USAFA, CO 80840, 1988) was employed, using a MNDO PM3 Hamiltonian with a restricted Hartree–Fock calculation, to obtain the heats of formation of the various S_xN_y intermediates. The heats of formation, as given in Ref. 12, at 298 K are ΔH_f (kcal mol^{-1}) = 81.2, 117, 54, 112.3, 54.8, and 98 for c-S_4N_4, a S_4N_4, c-S_3N_3, a-S_3N_3, c-S_2N_2, and a-S_2N_2, respectively.
[29] R. Bellman, G. Birnbaum, and W. G. Wagner, J. Appl. Phys. **34**, 780 (1963).
[30] C. B. Moore, J. Chem. Phys. **43**, 2979 (1965).
[31] A. G. Turner and F. S. Mortimer, Inorg. Chem. **5**, 906 (1966).
[32] We are grateful to Professor Gilbert Mains for carrying out the all electron *ab initio* calculations at the HF/6-31G* level at NCSA under Grant No. CHE890003N.
[33] M. Goehring, *Ergebnisse und Probleme d. Chemie der Schwefelstickstoff Verbindungen* (Akademie-Verlag, Berlin, 1957).
[34] R. D. Smith, Chem. Phys. Lett. **55**, 590 (1978).